Metrol. Meas. Syst., Vol. 30 (2023) No. 4, pp. 737–754
DOI: 10.24425/mms.2023.147960

PAN POLSKA AKADEMIA NAUK

METROLOGY AND MEASUREMENT SYSTEMS
Index 330930, ISSN 0860-8229
www.metrology.wat.edu.pl

M&MS

A YAW TRACKING ALGORITHM FOR HEAD MOVEMENT FROM INERTIAL SENSORS DATA

Anna Borowska-Terka, Paweł Strumiłło

Łódź University of Technology, Faculty of Electrical, Electronic, Computer and Control Engineering, Institute of Electronics, Al. Politechniki 10, 93-590 Łódź, Poland (✉ *anna.borowska-terka@p.lodz.pl, pawel.strumillo@p.lodz.pl*)

Abstract

Monitoring head movements is important in many aspects of life from medicine and rehabilitation to sports, and VR entertainment. In this study, we used recordings from two sensors, i.e. an accelerometer and a gyroscope, to calculate the angles of movement of the gesturing person's head. For the yaw motion, we proposed an original algorithm using only these two inertial sensors and the detected motion type obtained from a pre-trained SVM classifier. The combination of the gyroscope data and the detected motion type allowed us to calculate the yaw angle without the need for other sensors, such as a magnetometer or a video camera. To verify the accuracy of our algorithm, we used a robotic arm that simulated head gestures where the angle values were read out from the robot kinematics. The calculated yaw angles differed from the robot's readings with a mean absolute error of approx. 1 degree and the rate of differences between these values exceeding 5 degrees was significantly below 1 percent except for one outlier at 1.12%. This level of accuracy is sufficient for many applications, such as VR systems, human-system interfaces, or rehabilitation.

Keywords: yaw angle, gesture recognition, electronic human-machine interface, inertial sensors, IMU.

1. Introduction

Human beings, their physical capabilities and behaviour have always been the focus of researchers' attention. With the development of technology, the possibility of observing human behaviour has increased and the possibilities of applying such knowledge have expanded.

Miniaturisation, improved access to and lower cost of electronics facilitated the application of inertial sensors to track human activity. A smartphone, which arguably is the most popular personal device, with an appropriate application installed, can be used to track individual sleep patterns. Sensors built into sports bracelets and smartwatches not only can track the regularity of sleep, but can also be instrumental in increasing physical activity and monitoring the effectiveness of sports activities and weight control [1]. A whole range of sensors, including cameras, inertial sensors, and infrared sensors, are employed in VR devices typically used for entertainment, *e.g.*

Article history: received May 19, 2023; revised August 31, 2023; accepted September 11, 2023; available online November 21, 2023.

to boost engagement in playing a game or to enable watching movies in a virtual environment. These devices have also been applied in medicine [2]. In 2014, the first VR surgery was performed by Shafi Ahmed, who used VR googles during the operation, which allowed other viewers to remotely observe the operation on-line [3]. Video cameras – both single cameras and systems of cameras are among the most popular devices for tracking human physical activity. They make it possible to observe a single person as well as a whole group of people. Tracking human physical activity with a camera has been employed in various fields [4]. To improve road safety, a camera aimed at a driver can monitor his/her fatigue and tiredness. Combined with inertial sensors, cameras have been used to assist medical and physical therapy procedures. Finally, video cameras together with other sensors are also integrated in *Human-Computer Interfaces* (HCIs) to assist people with sensory and motor disabilities [5].

One type of movement that scientists are interested in is that of the head. Knowing the angle of rotation of the human head is important in many areas, including medicine and rehabilitation for nerve and muscle damage in the cervical spine, as an aid for people with disabilities, in sports to help athletes better control their bodies, or in the development of virtual reality entertainment such as films, computer applications and games to provide an appropriate user interface. Cameras can observe a person's head [6, 7] or they can be attached to the person's head [8]. Inertial sensors and sensors for motion/facial capture attached to the head have also been used to determine head movements [9]. Such sensors are embedded in VR goggles to track head motions. These movements can be tracked by calculating the following three angles, *i.e.*, yaw, roll, and pitch. The yaw angle is particularly difficult to track due to rotation around the vertical axis parallel to the gravity vector. In the case of roll and pitch movements, a fusion of signals received from the gyroscope and accelerometer is very often exploited. Since accelerometer signals are useless in determining yaw movements (motion around the gravity vector), this sensor is usually substituted with a magnetometer. One disadvantage here is that a magnetometer is a sensor that needs to be added to the system. It may also give incorrect readings as it is sensitive to nearby electronic devices and ferromagnetic materials [10, 11].

The contribution of this paper is validation of the method for tracking head movements of a seated person as defined by pitch, roll and yaw angles. To calculate the yaw angle, we propose an original algorithm that uses signals from only two types of sensors: the accelerometer and gyroscope that are attached to the person's forehead. In the proposed method the type of head movement is recognised first. Then the yaw angle can be confidently tracked from the gyroscope readings and the value of the yaw angle can be calculated. The advantage of our approach is that there is no need to incorporate into the tracking systems any data other than data from inertial sensors. To the best of the authors' knowledge, in other reported studies a magnetometer or video cameras had to be used to achieve sufficiently accurate tracking of the yaw angle of the person's head [12–14].

The remainder of this paper is organized as follows: Section 2 presents the research work related to head movement recognition. Section 3 introduces our algorithm, which is implemented in Section 4. Section 5 reports the experimental results and discussion about the advantages and disadvantages of the proposed yaw angle estimation algorithm. Finally, in the concluding Section 6, we summarize and discuss the results.

The abbreviations used in this paper: VR: Virtual Reality, SVM: Support Vector Machine, IMU: Inertial Measurement Unit, DTW: Dynamic Time Warping, HCIs: Human-Computer Interfaces, LED: Light Emitting Diode, deg/s: degrees/second, rad/s: radians/second, MSE: Mean Squared Error, RMSE: Root Mean Squared Error, MAE: Mean Absolute Error, ME: Max Error, MedAE: Median Absolute Error, WAD: Whiplash-associated disorders.

Metrol. Meas. Syst., Vol. 30 (2023), No. 4, pp. 737–754
DOI: 10.24425/mms.2023.147960

2. Related Work

The research on head movement tracking and recognition has been ongoing for years. It is carried out in many fields but many studies have focused in particular on medical applications. Recognition of head movements can be applied to assist people with physical dysfunctions, *e.g.* many studies describe the different ways in which individuals with disabilities can control their wheelchairs with head movements [7, 15–18]. In [15] and [17], signals from an accelerometer sensor were used to control the wheelchair. The accelerometer was attached to the top of the user's forehead. Head movements: tilt left, tilt right, keep head in natural position, were recognised based on the signals recorded from the sensor. Similarly in [18], researchers used an inertial sensor and the *dynamic time warping* (DTW) method to check for similarity between the two signals, which allowed for more complex gestures to be utilized in controlling the wheelchair, *e.g.*, head movement as if drawing a circle with the nose. In [16], signals from four capacitive sensors, evenly positioned around the neck, were used with the recognition of head movements based on the classification of the features extracted from the signals. In [7], a camera was used to observe head movements of a person in a wheelchair. Only the detection of both the head and the eyes made it possible to recognise the position of the head and control the wheelchair. The authors of the study [19] used head movements to remotely control a robot car. To properly control such a vehicle, its operator received a view of the road from a camera mounted on the robot car via streaming to VR goggles.

Head movements can also be used to control a robotic arm by tetraplegic users [8], to control a robot [12], or simply to move a pointer across a monitor screen [14]. Further, a personal gesture communication assistant based on head movements has been developed to facilitate communication for people with motor and speech impairments [6].

In 1967 Albert Mehrabian, a body language researcher, first unfolded the components of face-to-face conversation. He discovered that communication consists of 55% non-verbal elements, 38% vocal ones, with words accounting for a meagre 7% [20, 21]. From his studies came the belief that the dominant part of human communication is non-verbal. Hence, research was conducted on understanding the user's intention based on speech and simultaneous observation of head movements and apply this knowledge to robots that support elderly and lonely people [22]. In [23], the authors assessed the degree of stress by analysing head movements and the speed of movements during speaking. Head movement monitoring has also been successfully applied in assessing progress in the therapy of individuals suffering from depression. The method involved tracking head movements of the patient while he/she was talking to the doctor/therapist [24].

Another application of head movement tracking is to monitor eating behaviour. In [25] signals from the accelerometer combined with signals from the wrist-worn accelerometer were used to detect the time and frequency of the user's eating habits.

Drivers can benefit from head movement tracking to measure the level of fatigue they experience. To this end, both the driver's eyes and his/her head movements are observed [26, 27].

Another research area where head movements are explored is user authentication. Head movements detected by an accelerometer were fused with the torso movements recorded by a smartphone [28]. Knowing that free-style head movements in response to a fast beat audio track are characteristic and repetitive for individual users, in [29], the researchers were able to demonstrate that users can be authenticated by their distinctive head response to musical stimuli. In [9], a method for speaker identification was proposed that is based on the information encoded in the speaker's head gestures during storytelling.

Virtual reality (VR) technology, where head movement is the basis of VR performance [13, 30, 31] is another strongly growing field. The paper [30] focused on users' ability to redirect

walking manipulations, *i.e.* it investigated how the movement of the displayed scene and the movement of the user himself/herself influenced their perception of movement in workspace. In [13] and [31], the focus was on orientation drifts around the yaw axis. The researchers tracked when cumulative yaw drifts were acceptable and when they became uncomfortable to the user, and proposed a method for minimising these drifts.

The results of a number of research and scientific studies on head movements have been applied in commercial devices, such as Oculus Rift S [32], Sony PlayStation VR [33] and HTC VIVE Cosmos [34].

To calculate the roll and pitch angles, signals from the accelerometer and gyroscope are fused, whereas to calculate the yaw angle a fusion of signals from a gyroscope and a magnetometer is most often used [35, 36]. For VR goggles, inertial sensors information is additionally corrected based on camera data. Finally, when it comes to commercial devices [32–34], a large variety of sensors are used. Apart from inertial sensors, there are various types of cameras, proximity sensors, infrared sensors, infrared LEDs and laser position sensors. In [37], a VR stream tracker was designed to track only the movement of VR googles. Here, the so-called lighthouse tracking system was used. It consists of a base station emitting laser radiation and a set of sensors placed on the tracker.

A recent paper [38] proposed to calculate the yaw angle based on data from only one sensor, the accelerometer. The accelerometer, which rotates clockwise around the yaw axis only, is rigidly mounted on a flat Stewart Platform, and the radius r, *i.e.*, the distance of the accelerometer position from the axis of rotation, is known. Additionally, the most precise results were obtained for angles not exceeding 10°, while the largest errors (the error percentage value 8.21%) were obtained for the largest angles measured *i.e.* 60°. For humans these are important limitations, because human heads differ in head circumference, *i.e.*, the value of radius $r$varies. Also, as the head rotates, the sensor may not rotate exactly around the axis parallel to the gravity vector. These limitations as well as previous studies [12, 13, 31, 38] that used both inertial and other sensors to track human head movements, led us to propose a new approach based solely on inertial sensors recordings.

3. Materials and Methods

In our work we used a Duo MLX device [39]. It is equipped with a miniature camera, a 3-axis gyroscope, and a 3-axis accelerometer. The Duo MLX is of small dimensions (52x25x13mm) and low weight (12.5 g). These properties, *i.e.* negligible weight and small size, allowed us to employ it in our earlier study [40] where we placed the device on the forehead of a sitting person (see Fig. 1). The individual's task was to perform certain head movements which were recorded by an embedded gyroscope and accelerometer. The experiment with the Duo MLX device placed on the volunteer's forehead was approved by the bioethics commission of the Medical University of Łódź (No. RNN/261/16/KE).

The aim of study reported in [40] was to automatically classify three basic head gestures: pitch (head movement "up-down", Fig. 1d), roll (head movement "sideways", Fig. 1c), yaw (head movement "left-right", Fig. 1b), and immobility when the head remained at rest (Fig. 1a). 65 participants took part in the study. During the head movement recordings of the gyroscope and accelerometer signals, each person sat straight on a chair, had the Duo MLX rigidly attached to their forehead, and did not change the position of the device mounted on their forehead. Each participant had to perform a specific sequence of head movements containing combinations of the following movement types: pitch, roll, yaw, and immobility of varying duration. The recordings comprised sets of 6 element vectors. Each vector contained 3 signals from the accelerometer

Metrol. Meas. Syst., Vol. 30 (2023), No. 4, pp. 737–754
DOI: 10.24425/mms.2023.147960

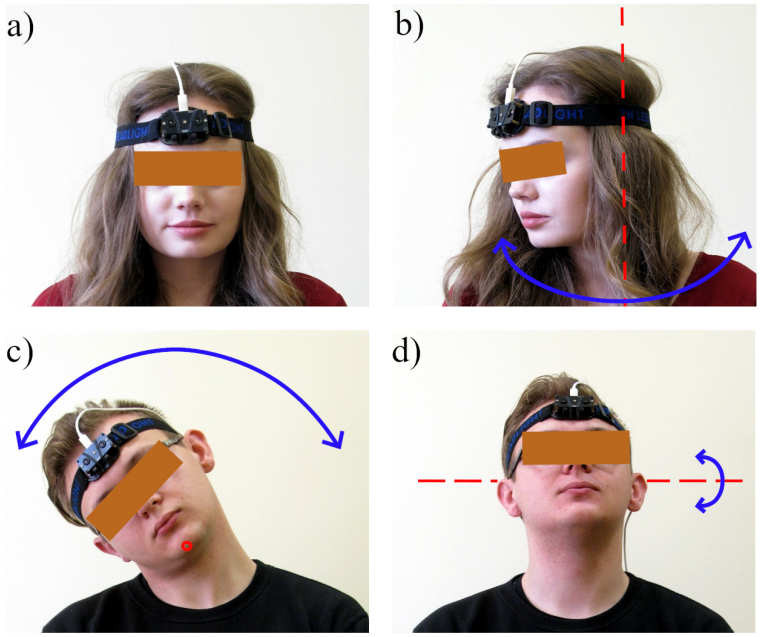

Fig. 1. Placement of the inertial measurement unit Duo MLX on the user's head, and types of head movements: a) immobility, b) yaw, c) roll, d) pitch. The blue colour indicates the direction of the head movement, whereas the red colour indicates the axis of rotation for the head movement.

and 3 signals from the gyroscope. The sampling rate was 100 Hz. The training set consisted of recordings from 53 individuals, while the test set comprised recordings from 12 participants. To classify head gestures based on the recorded IMU signals, the following data classifiers were used: a decision tree, a random forest, the *k-Nearest Neighbours* method (k-NN) and Support Vector Machines. The results of that study showed that by using raw signals from the inertial sensors mounted on the forehead of a sitting person, we can discriminate with an accuracy of 95% the type of head movement the person is making [40]. In this work, we build on our results and use the trained classifier for which we have achieved the best results, *i.e.*, *the Support Vector Machine* (SVM) classifier with a *radial basis function* (RBF) kernel and regularization parameter C = 10.0.

In the case of inertial sensors used for tracking head movements, data fusion is commonly applied to determine angles for yaw, pitch, and roll movements, *i.e.* the complementary filter [41, 42], Kalman filters [41], and particle filters [43].

To track the pitch and roll movements, we fused the gyroscope and the accelerometer signals by applying the Kalman filter.

A Kalman filter can also be used to determine the yaw motion. In this case, the signals from the accelerometer are not suitable, because for the yaw motion, the rotation of the head takes place approximately around an axis parallel to the gravity vector (the action of the acceleration of the earth). Consequently, for this motion, the signals obtained do not reflect the movement performed and are very close to the signals recorded during head immobility. This effect is illustrated in Fig. 2.

For the yaw angle estimation, the signals recorded by the gyroscope and magnetometer are often used and processed by a Kalman filter [35, 36]. However, readings from the magnetometer

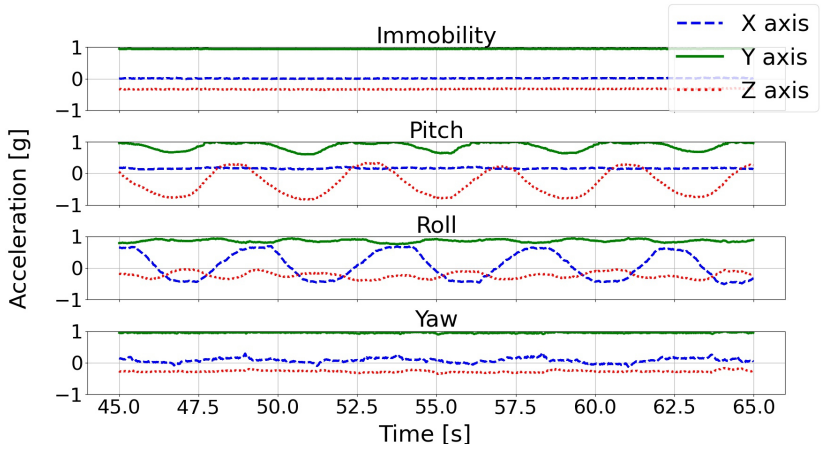

Fig. 2. Plots of 3-axis accelerometer signals from the Duo MLX device for various head movements.

can be interfered with by the nearby electronic devices and ferromagnetic objects and thus can yield incorrect readings [10, 11]. In our approach we use signals from inertial sensors only. Note, however, that the gyroscope data alone are insufficient. The gyroscope data are subject to errors and the calculated angles from the gyroscope signals are distorted by a drift, as shown in Fig. 3.

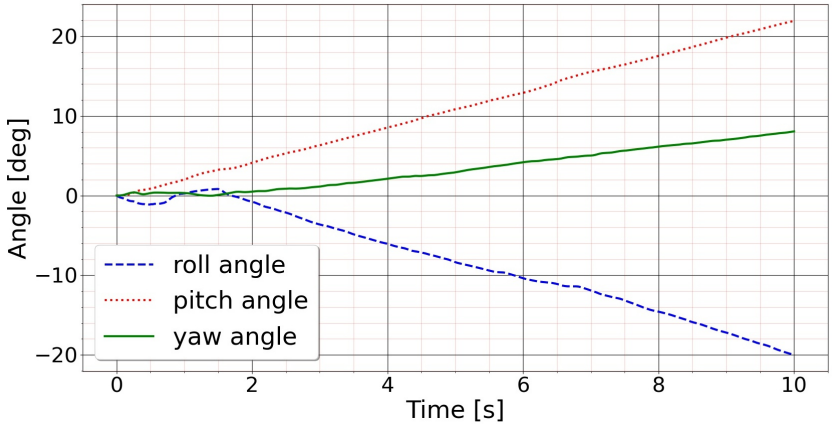

Fig. 3. Calculated angles based on signals from the gyroscope for a motionless sensor showing the drift.

To estimate the yaw angle, we propose a simple algorithm to calculate the direction of the head movement and the value of the yaw angle. For this purpose, we use the angle value calculated from the signals read only from the gyroscope and the recognized motion type obtained using the previously trained classifier. These two types of data, *i.e.*, the angle value and the detected motion type combined, allowed us to estimate the yaw angle.

The proposed algorithm for estimating the yaw angle consists of two parts: a) calculation of the yaw angle value when the detected motion is yaw, and d) correction of the yaw angle when the detected motion is immobility (see Fig. 4). Algorithm steps b) and c) are calculations of pitch and roll angles using the Kalman filter.

Metrol. Meas. Syst., Vol. 30 (2023), No. 4, pp. 737–754
DOI: 10.24425/mms.2023.147960

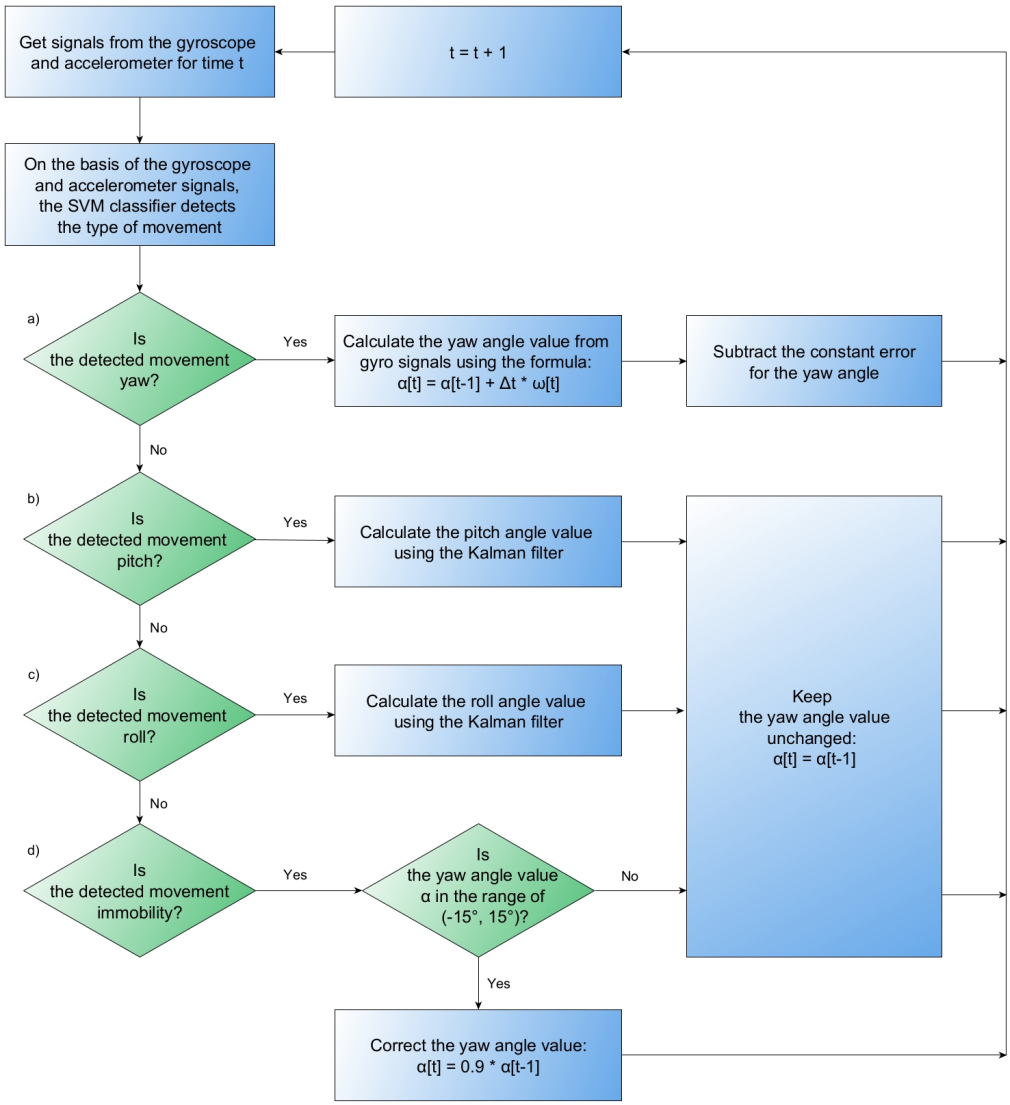

Fig. 4. Block diagram of the algorithm for estimating yaw, pitch, and roll angles.

3.1. Calculating the yaw angle

The yaw angle is calculated from the formula:

$$\alpha(t) = \alpha(t-1) + \omega(t) * \Delta t, \tag{1}$$

where:
$\alpha(t)$ – is the yaw angle value at the current time t,
$\alpha(t-1)$ – is the angle value at the previous sampling time $t-1$,
Δt – is the sampling period,
$\omega(t)$ – is the angular velocity read from the gyroscope at time t.

Figure 3 shows drifts in the gyroscope readings for a motionless sensor. These drifts follow nearly linear functions. Therefore, the calculated yaw angle is corrected by the constant determined value. This constant error was obtained by calculating the average drift error for 30s of the recording when the Duo MLX sensor was placed on the user's head in the immobility state.

The graph in Fig. 5 shows how the proposed algorithm for calculating the yaw angle of a seated person's head (red plot) compares to the calculation of the yaw angle based on the gyroscope signals only (green dashed plot). Note the clearly visible drift in the gyroscope readings. The plots correspond to sideway head movements within the range of 56°.

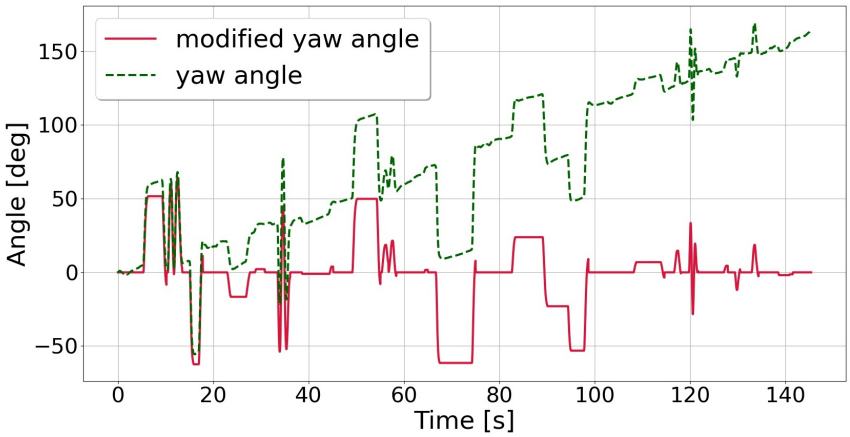

Fig. 5. Calculated yaw angles: green – based on signals from the gyroscope, red – the yaw angle calculated using the proposed algorithm.

3.2. Yaw angle correction for detected immobility

Yaw angle correction was also applied when the type of movement was head immobility and, at the same time, the value of the yaw angle was in the range of (–15°, 15°). When these conditions were met, the yaw angle was scaled down by a factor 0.9 (see Conditional Block d) in Fig. 4). The magnitude of the yaw angle in the interval (–15°, 15°), when immobility was detected, was treated as a value to be corrected and brought closer to 0. In that case, multiplying the size of the yaw angle by a factor of 0.9 was intended to reduce it.

The choice of the yaw angle in the interval (–15°, 15°), was motivated by the results presented in studies on VR systems [13, 30, 31]. It was shown that for a VR user, the orientation drift, *i.e.*, a shift of the virtual image relative to the real image, began to be perceived for values averaging 13°–25° [13, 31]. Additionally, when users were not focusing on the drift itself, they noticed a shift into the VR display relative to the real scene for angles exceeding ±19°. The paper [30] focused on introducing small shifts into a VR display to change the user's perception of distance and orientation in VR. It was found that if the drift had not exceeded 17°, the user did not notice it. Based on the results above, we used a value of ±15° in our work.

Figure 6 shows the value of the yaw angle depending on the value of the correction factor. For small values of the factor, the yaw angle correction occurs rapidly. On the other hand, for higher values of the factor *e.g.* 0.95, the correction occurs slowly and takes almost 1s. In determining the size of the factor value, it was assumed that the SVM classifier recognised types of movement with

95% accuracy, which meant that not every recognition of immobility was correct, and therefore an abrupt correction of the yaw angle value would also be incorrect. By choosing this factor close to 1, *i.e.*, 0.9, we maintained the yaw angle correction at a stable level, *e.g.*, in the case of an incorrect recognition of immobility, the yaw angle was not abruptly reduced to 0°. For the correction factor of 0.9, the correction of the yaw angle value is neither abrupt nor too slow – it occurs in less than 0.5 s.

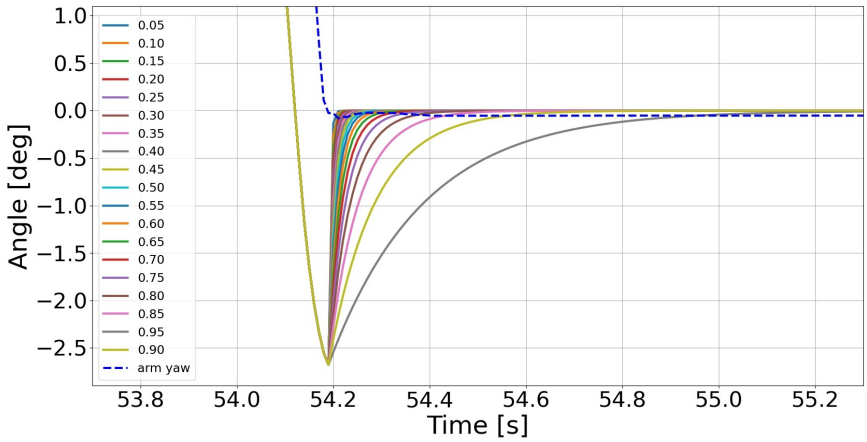

Fig. 6. Calculated yaw angles: dashed line – based on signals from the robot arm, solid line – the yaw angle calculated according to the proposed algorithm for different values of the correction factor.

The scripts implementing the described algorithm were written in Python. The open access Scikit-learn [44] module was used to train the SVM classifier.

4. Implementation and the validation of the algorithm

To verify the proposed method of calculating the yaw angle additional recordings were made using a robotic arm. The device we used was a Kuka LBR iiwa 14 R820 robot [45], which is a 7-axis robot arm. The repeatability of its pose is ±0.15 mm and the positioning accuracy is ±0.1 mm. In the case of the robot arm, the angles of rotation are calculated based on the position of each axis/joint which are read from an encoder coupled to the joint. Once the angle of rotation of each joint has been identified, the global orientations are determined based on the manipulator kinematics.

To test our algorithm, simulated head movements were recorded simultaneously for the robotic arm and the Duo MLX, ensuring that the recorded signals followed the same motion sequences. The Duo MLX was placed on the robotic arm as shown in Fig. 7. Both devices collected data at the same sampling rate of 100 Hz. The data obtained from the robotic arm were angle values given in radians. The data obtained from the Duo MLX were angular 3-axial velocities [rad/s] and accelerations [1 g = 9.8 m/s^2].

The Duo MLX device was placed on a special rack mounted on the axis/connector as shown in Fig. 7. The rack was designed to simulate the distance between the head and the neck – the places where the axes of rotation for the roll, pitch, and yaw movements occur.

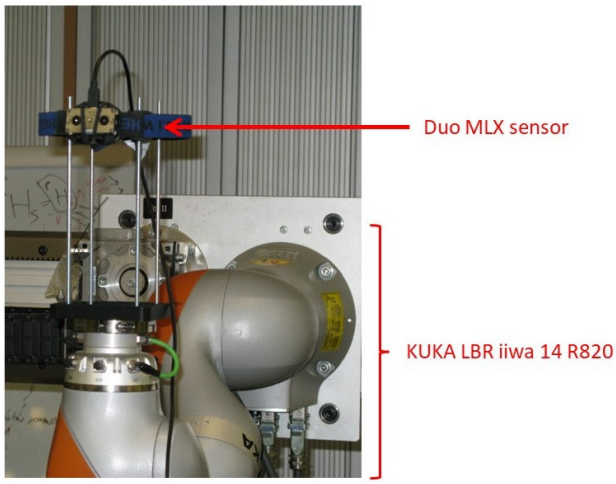

Fig. 7. KUKA LBR iiwa 14 R820 robot arm and Duo MLX sensor.

The movements of the robotic arm simulated the movements of the head as follows:

– roll – based on a rotation around axis 1, for which the possible range of movement is ±170°,
– pitch – based on a rotation around axis 4, for which the possible range of movement is ±120°,
– yaw – based on rotation about axis 7, for which the possible range of movement is ±175°.

The sensors from which the angles were read were in the flange (on Axis 7). The video showing Kuka LBR iiwa 14 R820 robotic arm with the Duo MLX device attached performing movements simulating the movements of the human head is available at [46].

To verify accuracy of the proposed method of calculating the yaw angle, seven test recordings were made using the robotic arm. The recording sequence was as follows: immobility – roll – immobility – yaw – immobility – pitch – immobility. The order of the movements was not important but the duration of a given movement was. The recording of the yaw movement, the focus of our work, lasted the longest, *i.e.*, 118 seconds, while pitch and roll movements were recorded at shorter intervals. As can be seen in Fig. 8, the robot performed only a few repetitions for the roll and pitch movements. As our method focuses on the yaw motion, there were many more repetitions of the yaw motion than of the other motions. The maximum yaw angles varied but they were always in the range of [–90°, 90°].

In the case of the robot, we have a constant angular velocity, whereas in the case of the human, the head movement is performed at varying speeds. However, it should be remembered that the movements of the robotic arm as well as the subjects' heads were calm and coordinated. There were no sudden and uncontrolled head movements.

In our previous work [40], we collected recordings of head movements from 65 participants. The maximum angular velocity that we observed was 250 deg/s (4.36 rad/s). The person who performed the slowest yaw movement had the highest angular velocity of 76 deg/s (1.33 rad/s). It should be emphasized that the provided maximum angular velocities were rarely recorded and were based on single samples. Some of the younger participants in our experiment were capable of moving their heads faster. However, during the recording of yaw movement sequences, subsequent repetitions were performed at a slower pace. The average yaw movement velocity across different participants ranged from 22 deg/s (0.38 rad/s) to 137 deg/s (2.39 rad/s).

Metrol. Meas. Syst., Vol. 30 (2023), No. 4, pp. 737–754
DOI: 10.24425/mms.2023.147960

5. Results and discussions

To verify the accuracy of the proposed algorithm, seven recordings were made of the robotic arm moving at a maximum speed of 82 deg/s (1.43 rad/s) and average angular velocity of 13 deg/s (0.23 rad/s). Our focus was on slower yaw movements, given that our further work aims to address rehabilitation and support for visually impaired individuals, with whom the Institute of Electronics of the Łódź University of Technology collaborates.

Both the sensors in the Duo MLX and the sensors in the robotic arm were in the initial state, *i.e.*, at certain angles, in the motionless state. To make it easier to compare the angle values recorded by the robot arm with the angles calculated by our algorithm, the angle values have been shifted so that the figure shows values close to zero when the robot is in the motionless state (Fig. 8).

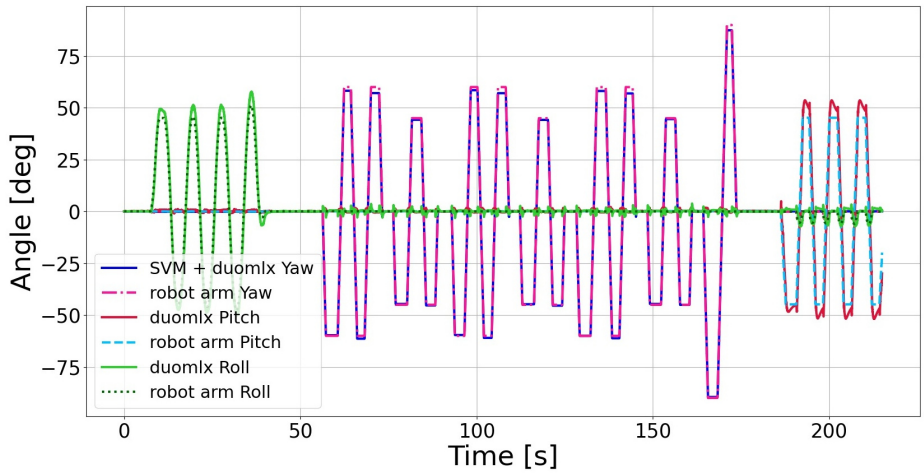

Fig. 8. Values of roll, pitch, and yaw angles recorded by the robotic arm (reference data) and the roll and pitch angles calculated by the Kalman filter based on the signals from the Duo MLX device, and the yaw angle calculated by the proposed algorithm.

Figure 9 shows the calculated angles during the yaw movement. The solid line shows the results obtained with our proposed algorithm, while the dashed line presents the readings from the arm angle. As can be seen from the graph, the two curves almost coincide.

To quantify the accuracy of the proposed algorithm, the following error measures were calculated for the yaw angles read from the robot arm and for the yaw angles calculated by the proposed algorithm:

– Mean Squared Error (MSE):

$$\mathrm{MSE}(y,\gamma) = \frac{1}{N_{\mathrm{samples}}} \sum_{i=0}^{N_{\mathrm{samples}}-1} (y_i - \gamma_i)^2 \tag{2}$$

– Root Mean Squared Error (RMSE):

$$\mathrm{RMSE}(y,\gamma) = \sqrt{\frac{1}{N_{\mathrm{samples}}} \sum_{i=0}^{N_{\mathrm{samples}}-1} (y_i - \gamma_i)^2} \tag{3}$$

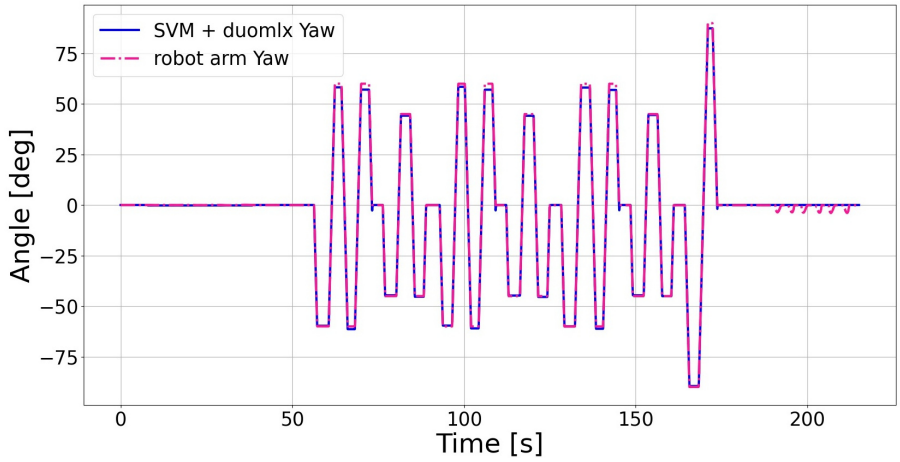

Fig. 9. Zoom in the Yaw angle values for maximum deflection obtained from the robot arm (reference data) and calculated using the proposed algorithm based on the signals from the Duo MLX combined with the results of the SVM classifier.

– Mean Absolute Error (MAE):

$$\mathrm{MAE}(y,\gamma) = \frac{1}{N_{\mathrm{samples}}} \sum_{i=0}^{N_{\mathrm{samples}}-1} |y_i - \gamma_i| \tag{4}$$

– Max Error (ME):

$$\mathrm{ME}(y,\gamma) = \max\left(|y_i - \gamma_i|\right) \tag{5}$$

– Median Absolute Error (MedAE):

$$\mathrm{MedAE}(y,\gamma) = \mathrm{median}\left(|y_1 - \gamma_1|, \ldots, |y_n - \gamma_n|\right). \tag{6}$$

The angle values measured with the robot arm were used as reference. The obtained results are presented in Table 1.

Table 1. Error measures of yaw angle differences between the reference values obtained from the robot arm system and the yaw angle values of the proposed algorithm.

Record No.	MSE [°]^2	RMSE [°]	MAE [°]	ME [°]	MedAE [°]
1	1.97	1.40	0.95	7.62	0.43
2	1.93	1.39	0.95	9.21	0.59
3	2.98	1.73	1.17	6.62	0.89
4	2.05	1.43	0.97	5.81	0.57
5	2.21	1.49	1.02	6.80	0.66
6	2.47	1.57	1.16	5.93	0.96
7	1.73	1.31	0.94	6.43	0.77

Note that the differences between the RMSE and MAE are small, which means that the variance of the distribution of individual errors in the recordings is also small. The largest ME

magnitude for individual recordings ranges from almost 6° to more than 9°. For the maximum tilts of the yaw angle, the maximum error was 3° for a deviation of 60°. For deviations of 45° and 90°, the errors obtained were less than 3°. Detailed analysis of the data showed that such large errors occurred only occasionally during the performance of the movement itself, *i.e.*, not at rest and not for the largest deviations.

Because we have considered the yaw motion in the range of [–90°, +90°], the ME values are quite large, but at the same time the MSE and RMSE magnitudes are small. The MSE and RMSE magnitudes are sensitive to large errors because they are calculated by squaring the error values. In our case, their small magnitudes indicate that there are not many large discrepancies between the yaw angle values obtained from the KUKA LBR iiwa 14 R820 robotic arm and those calculated according to our proposed method. In addition, the MedAE values, which unlike the MSE and RMSE are robust to outliers, do not exceed 1°. Therefore, half of the errors that occur do not exceed 1°. Considering yaw motion in the range of [–90°, +90°] the calculated MAE values are very small and oscillate around 1°.

Detailed analysis of the data showed that large errors close to the ME values occurred infrequently. In addition to the small magnitudes of MSE and RMSE, which are indicative of a small number of large errors, we also determined the percentage of large errors in the recordings. To do this, we calculated for what portion of the samples from the 7 recordings the difference between the yaw angles obtained from the KUKA LBR iiwa 14 R820 robot arm and the yaw angles calculated by our proposed method was greater than 5°. The results are presented in Table 2.

Table 2. Percentage of samples for which the difference between the reference values obtained from the robot arm system and the yaw angle values calculated by the proposed algorithm is greater than 5°.

Record No.	**Percentage of errors larger than 5° [%]**
1	0.15
2	0.34
3	1.12
4	0.30
5	0.21
6	0.46
7	0.20

We decided to calculate the angle differences larger than 5°, because for recording No. 4, the ME value was 5.81°. Therefore, to consider the differences in the yaw angle values from each record, we had to choose a discriminating value smaller than ME.

The calculated error measures from Table 1 and the magnitudes from Table 2 indicate that large errors are very rare. Furthermore, the low values of MAE, MSE, RMSE and MedAE suggest that our proposed method is robust.

Nevertheless, the proposed algorithm still requires further validation and improvements. The authors are aware that the proposed algorithm may not yield optimal results under specific conditions. This scenario occurs when the person's head remains immobile for a longer period within the small yaw angle range of (–15°, 15°). In such cases, the yaw angles are successively reduced by a factor of 0.9 in each iteration step of the algorithm (as explained in Section 3.2), resulting in a slightly different final value compared to the true one. If the yaw angle is within the aforementioned range, and simultaneously, the SVM classifier detects immobility for more

than a second in successive samples, the yaw angle will be reduced to a value close to zero. The selection of this procedure was motivated by VR applications of head tracking algorithms [13,31], where authors strove to detect clear and unambiguous gestures, *i.e.*, the difference between the calculated yaw angle and its true value did not exceed the range of (–15°, 15°).

Thank to it range, the motion tracking system may find medical applications. A very common type of injury in road traffic collisions is neck injury known as *whiplash-associated* disorders (WADs). It is characterised by changes in the extensor muscles and the muscle morphology of the cervical flexors, pain, loss of strength and endurance of the cervical muscle groups [47]. WAD are annoying and often long-lasting. Pain and muscle weakness in the cervical region can persist for years [48], and patients need to perform physical exercises, including range-of-motion exercises.

In our further work, we plan to use our results to create an interface to support physiotherapy for people with WAD. We also want to develop the interface into a mobile travel assistance system for visually impaired people [49].

6. Conclusions

The following conclusions can be drawn from the study:

1. It is possible to calculate the yaw angle using only the signals from one sensor, *i.e.* the gyroscope, provided that two sensors are used: a gyroscope and an accelerometer. To obtain an accurate estimate of the yaw angle, it was sufficient to augment the signals from the gyroscope with the type of movement that was recognised by a classifier based on the signals from two sensors: the gyroscope and the accelerometer (please refer to our earlier work reporting the results applying data classifiers to recognition of head gestures [40]).
2. The proposed algorithm was validated on reference angle measurements carried out with a Kuka LBR iiwa 14 R820 robotic arm. The maximum errors, depending on the recording, ranged from almost 6° to over 9°. However, such significant errors occurred sporadically. This is indicated by the percentage of errors larger 5°, which varied between 0.15 and 1.12 for individual recordings. The MedAE values, which are robust to outliers, do not exceed 1°. Consequently, half of the occurring errors do not surpass 1°. Very small percentage of large errors and low MAE, MSE, RMSE and MedAE values indicate that our proposed method is robust.
3. The advantage of the proposed angle calculation method is its simplicity. Moreover, only two inertial sensors were used in the study. The method does not require application of any calibration procedure as is the case for sensors used in VR goggles [32–34].

Acknowledgements

We would like to thank the staff of the Institute of Automatic Control of Łódź University of Technology, in particular prof. Grzegorz Granosik and Łukasz Chlebowicz, M.Sc., for providing access to the robot arm KUKA LBR iiwa 14 R820, and for their assistance in carrying out the measurements.

References

[1] Roomkham, S., Lovell, D., Cheung, J., & Perrin, D. (2018). Promises and challenges in the use of Consumer-Grade devices for sleep monitoring. *IEEE Reviews in Biomedical Engineering*, *11*, 53–67. https://doi.org/10.1109/rbme.2018.2811735

[2] Buettner, R., Baumgartl, H., Konle, T., & Haag, P. (2020, July). A Review of Virtual Reality and Augmented Reality Literature in Healthcare. In *2020 IEEE Symposium on Industrial Electronics & Applications (ISIEA)* (pp. 1–6). IEEE. https://doi.org/10.1109/ISIEA49364.2020.9188211

[3] Shafi Ahmed. (2023, November 10). In *Wikipedia*. https://en.wikipedia.org/wiki/Shafi_Ahmed

[4] Aggarwal, J. K., & Ryoo, M. S. (2011). Human activity analysis. *ACM Computing Surveys*, *43*(3), 1–43. https://doi.org/10.1145/1922649.1922653

[5] Mahmud, S., Lin, X., & Kim, J. H. (2020, January). Interface for human machine interaction for assistant devices: A review. In *2020 10th Annual Computing and Communication Workshop and Conference (CCWC)* (pp. 0768–0773). IEEE. https://doi.org/10.1109/CCWC47524.2020.9031244

[6] Ascari, R. E. S., Silva, L., & Pereira, R. (2020, March). Personalized gestural interaction applied in a gesture interactive game-based approach for people with disabilities. In *Proceedings of the 25th International Conference on Intelligent User Interfaces* (pp. 100–110). https://doi.org/10.1145/3377325.3377495

[7] Solea, R., Margarit, A., Cernega, D., & Serbencu, A. (2019, October). Head movement control of powered wheelchair. In *2019 23rd International Conference on System Theory, Control and Computing (ICSTCC)* (pp. 632–637). IEEE. https://doi.org/10.1109/ICSTCC.2019.8885844

[8] Kyrarini, M., Zheng, Q., Haseeb, M. A., & Gräser, A. (2019, June). Robot learning of assistive manipulation tasks by demonstration via head gesture-based interface. In *2019 IEEE 16th International Conference on Rehabilitation Robotics (ICORR)* (pp. 1139–1146). IEEE. https://doi.org/10.1109/ICORR.2019.8779379

[9] Vadiraj, S. K., Rao, A., & Ghosh, P. K. (2020, May). Automatic Identification of Speakers From Head Gestures in a Narration. In *ICASSP 2020-2020 IEEE International Conference on Acoustics, Speech and Signal Processing (ICASSP)* (pp. 6314–6318). IEEE. https://doi.org/10.1109/icassp40776.2020.9053124

[10] Titterton, D., & Weston, J. (2004). *Strapdown inertial navigation technology* (2nd ed.). AIAA.

[11] Wu, Z., & Wang, W. (2018). Magnetometer and gyroscope calibration method with level rotation. *Sensors*, *18*(3), 748. https://doi.org/10.3390/s18030748

[12] Rudigkeit, N., Gebhard, M., & Graser, A. (2015, December). An analytical approach for head gesture recognition with motion sensors. In *2015 9th International Conference on Sensing Technology (ICST)* (pp. 1–6). IEEE. https://doi.org/10.1109/icsenst.2015.7933064

[13] Feigl, T., Mutschler, C., & Philippsen, M. (2018, March). Human Compensation Strategies for Orientation Drifts. In *2018 IEEE Conference on Virtual Reality and 3D User Interfaces (VR)* (pp. 409–414). IEEE. https://doi.org/10.1109/VR.2018.8446300

[14] Jalaliniya, S., Mardanbeigi, D., Pederson, T., & Hansen, D. W. (2014, June). Head and eye movement as pointing modalities for eyewear computers. In *2014 11th International Conference on Wearable and Implantable Body Sensor Networks Workshops* (pp. 50–53). IEEE. https://doi.org/10.1109/BSN.Workshops.2014.14

[15] Dey, P., Hasan, M. M., Mostofa, S., & Rana, A. I. (2019, January). Smart wheelchair integrating head gesture navigation. In *2019 International Conference on Robotics, Electrical and Signal Processing Techniques (ICREST)* (pp. 329–334). IEEE. https://doi.org/10.1109/ICREST.2019.8644322

[16] Dobrea, M. C., Dobrea, D. M., & Severin, I. C. (2019, November). A new wearable system for head gesture recognition designed to control an intelligent wheelchair. In *2019 E-Health and Bioengineering Conference (EHB)* (pp. 1–5). IEEE. https://doi.org/10.1109/EHB47216.2019.8969993

[17] Nasif, S., & Khan, M. A. G. (2017, December). Wireless head gesture controlled wheel chair for disable persons. In *2017 IEEE Region 10 Humanitarian Technology Conference (R10-HTC)* (pp. 156–161). IEEE. https://doi.org/10.1109/R10-HTC.2017.8288928

[18] Mavuş, U., & Sezer, V. (2017, March). Head gesture recognition via dynamic time warping and threshold optimization. In *2017 IEEE Conference on Cognitive and Computational Aspects of Situation Management (CogSIMA)* (pp. 1–7). IEEE. https://doi.org/10.1109/COGSIMA.2017.7929592

[19] Wee, T. J., & Wahid, H. (2021). Design of a Head Movement Navigation System for Mobile Telepresence Robot Using Open-source Electronics Software and Hardware. *International Journal of Electronics and Telecommunications*, 379–384. https://doi.org/10.24425/ijet.2021.137823

[20] Wiener, M. (1967). Decoding of inconsistent communications. *Journal of Personality and Social Psychology*, *6*(1), 109–114. https://doi.org/10.1037/h0024532

[21] Mehrabian, A., & Ferris, S. R. (1967). Inference of attitudes from nonverbal communication in two channels. *Journal of Consulting Psychology*, *31*(3), 248. https://doi.org/10.1037/h0024648

[22] Kasano, E., Muramatsu, S., Matsufuji, A., Sato-Shimokawara, E., & Yamaguchi, T. (2019, June). Estimation of speaker's confidence in conversation using speech information and head motion. *In 2019 16th International Conference on Ubiquitous Robots (UR)* (pp. 294-298). IEEE. https://doi.org/10.1109/URAI.2019.8768561

[23] Giannakakis, G., Manousos, D., Simos, P., & Tsiknakis, M. (2018, May). Head movements in context of speech during stress induction. In *2018 13th IEEE International Conference on Automatic Face & Gesture Recognition (FG 2018)* (pp. 710–714). IEEE. https://doi.org/10.1109/FG.2018.00112

[24] Bhatia, S., Goecke, R., Hammal, Z., & Cohn, J. F. (2019, May). Automated measurement of head movement synchrony during dyadic depression severity interviews. In *2019 14th IEEE International Conference on Automatic Face & Gesture Recognition (FG 2019)* (pp. 1–8). IEEE.. https://doi.org/10.1109/FG.2019.8756509

[25] Ye, X., Chen, G., & Cao, Y. (2015, October). Automatic eating detection using head-mount and wrist-worn accelerometers. In *2015 17th International Conference on E-health Networking, Application & Services (HealthCom)* (pp. 578–581). IEEE. https://doi.org/10.1109/HealthCom.2015.7454568

[26] Hammoud, R. I., Wilhelm, A., Malawey, P., & Witt, G. J. (2005, June). Efficient real-time algorithms for eye state and head pose tracking in advanced driver support systems. In *2005 IEEE Computer Society Conference on Computer Vision and Pattern Recognition (CVPR'05)* (Vol. 2, pp. 1181-vol). IEEE. https://doi.org/10.1109/CVPR.2005.142

[27] Niyogi, S., & Freeman, W. T. (1996, October). Example-based head tracking. *In Proceedings of the second international conference on automatic face and gesture recognition* (pp. 374–378). IEEE. https://doi.org/10.1109/afgr.1996.557294

[28] Parimi, G. M., Kundu, P. P., & Phoha, V. V. (2018, January). Analysis of head and torso movements for authentication. In *2018 IEEE 4th International Conference on Identity, Security, and Behavior Analysis (ISBA)* (pp. 1–8). IEEE. https://doi.org/10.1109/ISBA.2018.8311460

[29] Li, S., Ashok, A., Zhang, Y., Xu, C., Lindqvist, J., & Gruteser, M. (2016, March). Whose move is it anyway? Authenticating smart wearable devices using unique head movement patterns. In *2016 IEEE International Conference on Pervasive Computing and Communications (PerCom)* (pp. 1–9). IEEE. https://doi.org/10.1109/PERCOM.2016.7456514

[30] Steinicke, F., Bruder, G., Jerald, J., Frenz, H., & Lappe, M. (2008, October). Analyses of human sensitivity to redirected walking. In *Proceedings of the 2008 ACM symposium on Virtual reality software and technology* (pp. 149–156). https://doi.org/10.1145/1450579.1450611

[31] Feigl, T., Mutschler, C., & Philippsen, M. (2018, September). Supervised learning for yaw orientation estimation. In *2018 international conference on indoor positioning and indoor navigation (IPIN)* (pp. 206–212). IEEE. https://doi.org/10.1109/IPIN.2018.8533811

[32] Meta. Developer Forum. https://forums.oculusvr.com/t5/Oculus-Developer/ct-p/developer

[33] Nishino, H. (2022). PlayStation VR2 and PlayStation VR2 Sense controller: the next generation of VR gaming on PS5. *PlayStation.Blog*. https://blog.playstation.com/2022/01/04/playstation-vr2-and-playstation-vr2-sense-controller-the-next-generation-of-vr-gaming-on-ps5/

[34] HTC VIVE. *VIVE Developers |Get started developing for COSMOS*. https://developer.vive.com/us/hardware/vive-cosmos/

[35] Marins, J. L., Yun, X., Bachmann, E. R., McGhee, R. B., & Zyda, M. J. (2001, October). An extended Kalman filter for quaternion-based orientation estimation using MARG sensors. In *Proceedings 2001 IEEE/RSJ International Conference on Intelligent Robots and Systems. Expanding the Societal Role of Robotics in the the Next Millennium (Cat. No. 01CH37180)* (Vol. 4, pp. 2003–2011). IEEE. https://doi.org/10.1109/iros.2001.976367

[36] Witczak, A. (2015). FPV Headtracker inercyjny sterownik ruchu (1). *Elektronika Praktyczna*, (8), 16–25.

[37] Maciejewski, M., Piszczek, M., Pomianek, M., & Palka, N. (2020). Design and evaluation of a steamvr tracker for training applications – simulations and measurements. *Metrology and Measurement Systems*, *27*(4), 601–614. https://doi.org/10.24425/mms.2020.134841

[38] Nurhakim, A., Effendi, M. R., Saputra, H. M., Mardiati, R., Priatna, T., & Ismail, N. (2019, July). A Novel Approach to Calculating Yaw Angles Using an Accelerometer Sensor. In *2019 IEEE 5th International Conference on Wireless and Telematics (ICWT)* (pp. 1–4). IEEE. https://doi.org/10.1109/ICWT47785.2019.8978238

[39] DUO3D™Division. *DUO – Ultra-compact Stereo Camera for Sensing Space*, Retrieved May, 2023, https://duo3d.com/

[40] Borowska-Terka, A., & Strumillo, P. (2020). Person independent recognition of head gestures from parametrised and raw signals recorded from inertial measurement unit. *Applied Sciences*, *10*(12), 4213. https://doi.org/10.3390/app10124213

[41] Kok, M., Hol, J. D., & Schön, T. B. (2017). Using inertial sensors for position and orientation estimation. *Foundations and Trends in Signal Processing*, *11*(1–2), 1–153. https://doi.org/10.1561/2000000094

[42] LaValle, S. M., Yershova, A., Katsev, M., & Antonov, M. (2014, May). Head tracking for the Oculus Rift. In *2014 IEEE international conference on robotics and automation (ICRA)* (pp. 187–194). IEEE. https://doi.org/10.1109/ICRA.2014.6906608

[43] Ababsa, F., Didier, J. Y., Mallem, M., & Roussel, D. (2003, December). Head Motion Prediction in Augmented Reality Systems Using Monte Carlo Particle Filters. In *Proceeding of the 13th International Conference on Artificial Reality and Telexistence (ICAT 2003)*.

[44] Pedregosa, F., Varoquaux, G., Gramfort, A., Michel, V., Thirion, B., Grisel, O., Blondel, M., Prettenhofer, P., Weiss, R., Dubourg, V., Vanderplas, J., Passos, A., Cournapeau, D., Brucher, M., Perrot, M., & Duchesnay, É. (2011). Scikit-Learn. Machine Learning in Python. *Journal of Machine Learning Research*, 12, 2825–2830.

[45] KUKA AG. *LBR iiwa*. Retrieved May, 2023. https://www.kuka.com/en-gb/products/robotics-systems/industrial-robots/lbr-iiwa

[46] Anna Borowska-Terka. Retrieved May, 2023. http://eletel.p.lodz.pl/abterka

[47] Sterling, M. (2014). Physiotherapy management of whiplash-associated disorders (WAD). *Journal of Physiotherapy*, *60*(1), 5–12. https://doi.org/10.1016/j.jphys.2013.12.004

[48] Tournier, C., Hours, M., Charnay, P., Chossegros, L., & Tardy, H. (2015). Five years after the accident, whiplash casualties still have poorer quality of life in the physical domain than other mildly injured casualties: analysis of the ESPARR cohort. *BMC Public Health*, *16*(1). https://doi.org/10.1186/s12889-015-2647-8

[49] Caraiman, S., Morar, A., Owczarek, M., Burlacu, A., Rzeszotarski, D., Botezatu, N., Herghelegiu, P., Moldoveanu, F., Strumiłło, P., & Moldoveanu, A. (2017, January). Computer Vision for the Visually Impaired: the Sound of Vision System. In *Proceedings – 2017 IEEE International Conference on Computer Vision Workshops (ICCVW 2017)* (pp. 1480–1489). IEEE. https://doi.org/10.1109/ICCVW.2017.175

Anna Borowska-Terka received her M.Sc. degree in applied mathematics from Łódź University of Technology, Poland. She works as an IT specialist at the Institute of Electronics, Łódź University of Technology. Her research interests are signal processing and machine learning. She is currently working towards her Ph.D.

Paweł Strumiłło is a full-time university professor at Łódź University of Technology (TUL), Poland. His current research interests include medical electronics, biosignal processing, soft computing methods and assistive systems for the disabled. He has published more than 90 research papers and three books. Since 2015 he has been the head of the Institute of Electronics of TUL. He is a Senior Member of the IEEE and a member of the Biocybernetics and Biomedical Engineering Committee of the Polish Academy of Sciences.